Engineering a solution to the problem of dry-band arcing on ADSS cables

IEEE Electrical Insulation Magazine 22 Issue 4 (2006) 34 - 43

S M Rowland

DOI: 10.1109/MEI.2006.1678356

ENGINEERING A SOLUTION TO THE AGEING OF HV SELF SUPPORTING CABLES BY DRY-BAND ARCING

S. M. Rowland

The School of Electrical and Electronic Engineering, The University of Manchester, PO Box 88, Manchester, M60 1QD, UK

INTRODUCTION

Telecommunication and energy deregulation have made it attractive for power utilities to deploy optical fibres on their networks for telecommunication applications. Initially for their own use, this has extended to carrying traffic for third parties, and even leasing fibre. Many forms of cables are available for this [1,2]. One generic cable is generally known as all-dielectric self-supporting (ADSS) cable. This is an extension of traditional self-supporting optical cable designs which have been used on roadside wood-pole structures for many years, although typical high-voltage span lengths of over 300 m present additional challenges since metallic strength members are not used [1]. Instead pultruded glass-reinforced plastic or stranded aramid yarns are used for the strength element. Figure 1 shows the typical location of an ADSS cable on the lower cross-arm of a twin circuit tower.

Early deployment of ADSS cables at low voltages presented no problems, but at high voltages unexplained failures occurred adjacent to the clamp arrangements. These were first informally reported in the mid 1980s . Since that time the principal mechanism of ageing has been identified as dry-band arcing [3,4]. The role of corona discharge at the earthed metallic cable clamps is one that continues to be investigated [5].

Generally the electrical severity of an installation site is referred to by the magnitude of the space potential in which the cable sits. This is not a sound approach, since it is the magnitude of currents

flowing on the cable that controls the damage mechanism. These currents are controlled by the nature of the local pollution and moisture on the cable in addition to the space potential in which the cable sits.

Several potential solutions have been proposed to this problem [6,7], although none other than improving sheath performance has been commercialized in large-scale installations. Sheath materials are used which resist degradation by dry-band arc activity. Unfortunately the issue of predicting cable lifetime remains unsolved for this approach. Nonetheless, experience suggests that a cable with a good dry-band arc-resistant material is satisfactory for most environments on systems up to 275 kV [8,9]. The debate on this continues, heavily influenced by commercial considerations, and complicated by the fact that cables have survived in some situations in very high fields for long periods of time.

Failures of installed cables are commercially sensitive, so problems and their resolutions are not generally published. This is now beginning to change and details of problems experienced in Israel are typical of what is reported informally [10]. Thus, there is still debate concerning the true severity of any threat, and consensus has yet to be reached on many aspects of failure.

A novel solution to the problems caused by dry-band arcing on ADSS cables is presented here, along with a description of the application engineering required to design a working system.

DRY-BAND ARCING ON ADSS CABLES

The origins of dry-band arcing on ADSS cables have been widely reported. A distributed capacitance exists between the dielectric cable, the ground and each of the individual conductors. This is shown schematically in Figure 2. This coupling results in a field gradient along the dielectric cable. The space potential is at a maximum at mid-span and is at ground potential at the towers, where the cable is grounded by metallic clamps. It is usual to describe the cable as dielectric, indicating a negligible conductivity per unit length, however in the event of rain,

pollution or an aged cable, the surface of the cable does become more conductive. This conductivity will allow currents to flow along the cable length, and will modify the field gradient on the cable surface. These currents are proportional to the voltage gradient and are normally greatest at the clamps and towers [4].

Joule heating will tend to dry a moist surface through which a current passes. The heating is proportional to the resistance per unit length of the cable, and so as the cable dries and becomes more resistive the heating increases and eventually one part of the cable will adventitiously dry out totally. This is the traditional concept of the formation of a 'dry band'. It is found that the length of any dry band will initially be similar to the diameter of the cable. The voltage across the dry band is proportional to the dry-band resistance per unit length, and ultimately its resistance can increase to the point where the voltage is so large that an arc can be struck. This is the dry-band arc. This situation is significantly different from that which occurs on most insulators however, because the current available to an arc is strictly limited. If moisture continues to be deposited by fog or rain, the balance of Joule heating and moisture deposition will determine whether the dry band is smothered with moisture, or continues to increase in length until the voltage is no longer sufficient to strike an arc.

The presence of arcs will damage traditional cable sheath materials. Arcing results in carbon tracks forming (for example with PVC), oblation of material (for filled EVA) or simple melting processes (for polyethylene). Which ageing mechanism tends to dominate depends upon the intensity of the arcing and the material concerned. Improvements have been made to the cable surface by producing improved polymeric compounds [8,11-13]. These materials have significantly enhanced the life expectancy of cables. Unfortunately ageing processes are not yet well enough understood to enable clear lifetime predictions to be made [14-16]. Nonetheless, cable manufacturers have sufficient confidence in their products to offer them into various situations. Virtually all manufacturers will offer cables onto 150 kV lines and below. Figures 3 and 4 show pictures of damage from installations on 400 kV and 110 kV lines respectively.

Currents experienced in service will typically peak between 1 and 5 mA in heavily polluted conditions. Unfortunately this is the worst case current for polymer degradation [17,18]. Thus the geometric capacitive limitation to the maximum current accelerates the ageing processes. A number of researchers have developed models enabling predictions of currents and fields experienced by each cable [4,19-22]. Typical results generated by such models are shown in Figure 5. Previously, a fully instrumented installation on a 400 kV line has shown consistency with the models developed [20]. In those measurements, confirmation of the dry-band arcing events correlating with high pollution and specific weather conditions were confirmed, as shown in Figure 6. One key parameter of any model is the choice of polluted cable conductivity. This clearly varies in time and with geography. Experience shows this can vary radically over a distance of a few kilometres within an installed section of cable. Because of the uncertainty about the resistance per unit length of any installed cable, the utilization of models to predict surface currents is very difficult.

The use of mid-span equipotential contours such as that shown in Figure 5 has become standard practice. In an ADSS application analysis, the space potential contour plot is studied in order to identify locations of low space potential, where the ADSS cable could be installed. Historically, a space potential contour of 12 kV and above was considered to represent locations within which an ADSS cable could become susceptible to damage by dry-band arcing [23]. Guidelines relating to the geographical location of the proposed ADSS installation were also created in an attempt to ensure that the currents on the cable were acceptably low. For example, Table 1, reproduced from Carter et al [24], shows a proposed estimation technique for relating the ‘safe’ space potential threshold level to the estimated resistance per unit length of the cable; above the threshold level, damaging arcing may reasonably be expected to occur.

Typically, in order to determine the ‘pollution level’, it is necessary to check whether the line is located near to a coastline or to a source of industrial pollution, as it is known that both of these

parameters can contribute to the ADSS cables becoming conductive, and hence susceptible to dry-band arc-related degradation.

Such analysis of space potential contours must however be complete. It is necessary to consider the effect of single circuit outages on twin circuit lines. Figure 7 shows that in such circumstances calculated potentials can rise significantly, as will associated currents. This is important because even if such outages last for a small fraction of time, it has been shown that aggressive ageing tends to occur in short periods, not gradually over the cable's life. Thus such outages combined with high pollution levels might combine to provide conditions necessary for severe arcing to take place.

THE RETRO-FIT ROD SOLUTION (ARC ARREST SYSTEM, AAS)

One of the methods proposed to alleviate the problem of dry-band arcing, is the introduction of conductivity into the cable [7]. The electrical field across a dry band depends upon the resistance of that band: it is the high resistance of that region compared to the rest of the cable which leads to a high field across the band and the resultant arc. If a dry band were to occur on a conductive cable, there would be a high conductivity component from the cable in parallel with the dry band, thus the electrical stress and so the total voltage dropped across it would be reduced, thereby preventing arcing from occurring.

The required conductivity in such a cable is determined by the resistivity of the polluted cable surface. The cable cannot be made too conductive since it is its dielectric nature which allows live-line installation and ensures clearances are maintained. Thus simply producing a cable with a sheath made from a standard 'semiconducting' carbon-loaded polymer is not a solution. Such materials typically have resistivity of 5 Ωm. For a cable of 14 mm diameter with a radial sheath thickness of 1.5 mm, this gives a cable of resistance per unit length 85 kΩ/m, much too conductive to be treated as insulating. It might be imagined that by reducing the conducting material thickness to 0.25 mm, a more suitable resistance per unit length would result. Unfortunately it is hard to control this value of conductivity during manufacture with traditional materials and extrusion

techniques, and processing such thin layers enhances the conductivity beyond calculated and acceptable values. Moreover, any region of the cable with an anomalously high resistance would threaten to create conditions of thermal runaway, since the cable would continuously draw current. Thus a poorly manufactured conductive cable will pose a more severe and immediate problem than a dielectric one.

If the minimum stable dry band length is controlled by the cable diameter and is taken as 10 mm, and the maximum current on a heavily polluted cable is 5 mA, then a cable with intrinsic resistance per unit length 1 MΩ/m could never have more than 5 kV/m along a dry section. This equates to 50 V over a 10 mm dry band, a voltage too low to cause arcing. The current of 5 mA would result in Joule heating in the sheath of 25 W/m. The balance of providing enough conductivity to prevent arcing, retaining the cable's dielectric nature for safety, and dissipating heat means that only a narrow window of cable resistivity is acceptable.

An alternative to making a cable with controlled resistivity is to introduce the conductivity after the dielectric cable is installed. One such solution, the arc arrest system (ASS), consists of a rod of controlled resistance per unit length which is attached to a previously installed ADSS cable [25]. The rod covers the first 50 m of the cable adjacent to the tower, and is earthed at the tower. The rod is held on by simple clips that enable it to be manually pushed on to the cable with no mechanical aids [20,26]. Figures 8 and 9 show this schematically. The rod consists of a glass reinforced plastic strength element sheathed with a conductive, carbon-loaded engineering polymer.

This post-fit approach has a number of advantages. The rod is manufactured separately from the cable, allowing independent quality control. A thin sheath provides control of the resistivity and because the rod is external to the cable sheath it is able to dissipate heat better and so take a higher current for equivalent temperature rise. The cable is installed as a dielectric cable using traditional techniques, and a range of conductivity rods can be made for different circumstances if necessary.

Because it is retro-fit, the rod can be installed some time after cable installation. It also only needs to be installed on the spans of cable which are at risk, reducing the system cost.

GENERIC SYSTEM DESIGN

The manner in which the rod works is to prevent significant voltage to be built up across a dry band, as in a conductive cable. The conductive rod does not need to be installed over the whole span length. In this situation a dry band can occur beyond the rod's length, and then the damage caused by an arc is limited by the reduced current available to the arc. Figure 10 shows the electrical model of the rod and cable. Essentially we assume the rod has a linear resistance of R_r per unit length and the cable (including pollution) has a resistance R_c per unit length. The clips are spaced every 30 cm, and are assumed to be conductive. This is reasonable since they are made of material much more conductive than the rod.

The maximum current seen in the whole system will generally be at the clamp, and this is shared between the rod and the cable surface. Each of the drawings in Figure 11 illustrates a different situation to be considered in the design. Here the cable is represented as a substrate for conductive pollution. We define zone 1 as that part of a half-span covered by the rod, and zone 2 as that region beyond the rod end to mid-span. For clarity, the clips are not shown in this diagram.

Figure 11(A) shows a dry cable with a resistive rod. The maximum current in this system at X is the current accumulated over zone 1, as shown in Figure 9. This is the minimum current ($i_{x\ dry}$) which the resistive rod will experience and must be endured over its lifetime. Joule heating is given by $(i_{x\ dry})^2\ R_r$, where R_r is the resistance per unit length of the rod. This heating is continuously generated and must not age the rod unacceptably. The limiting value depends upon the rod design. In the design considered we require:

$$(i_{x\ dry})^2\ R_r < 10\ \text{W/m} \qquad (1)$$

Figure 11(B) shows the situation when the cable is completely wet. The current is greater than in case 11(A). The current at X, $i_{x\ wet}$, will be shared between the rod and the moisture. Dry band formation will be slowed by the presence of the rod since the normal positive feedback effect of increasing resistance as moisture is dried will be reduced.

Figure 11(C) shows a dry band formed at the clamp end of the rod at X. The voltage gradient on the rod is increased across the dry band. This is because the current is virtually unaffected by the local increase in resistance. If the voltage across the dry band is sufficient, an arc will occur. The voltage available for an arc across the dry band is given by the product of $i_{x\ wet}$, R_r and the dry band width. To ensure an arc cannot strike we require that:

$$i_{x\ wet}R_r < 10\ \text{kV/m} \tag{2}$$

$i_{x\ wet}$ is also the maximum current the rod may have to endure for short periods of Joule heating. In this case we require:

$$(i_{x\ wet})^2R_r < 40\ \text{W} \tag{3}$$

This short-term heating limit also depends on the rod design. The current available for an arc in this location is the share of $i_{x\ wet}$ carried on the cable sheath, $i_{xc\ wet}$, rather than in the rod. To ensure the sheath is not damaged this current must not be too large. For the sheath material considered here we require that if condition (2) is not met then:

$$i_{xc\ wet} < 1.0\ \text{mA} \tag{4}$$

Figure 11(D) shows a dry band within the length of the rod, at Y. If R_r is well controlled and constant along the rod length, this situation must be less onerous than at a dry band at X, since the current must be lower. In real systems, local variations in R_r must be expected, and the key to manufacturing such a rod is ensuring this variation is within acceptable limits so that Joule heating is tolerable, and the voltage across such gaps is controlled satisfactorily.

The case shown in Figure 11(E) is similar to that in (A). The primary difference is that a current, i_z, can now flow through the tip of the rod from the rest of the span at point Z. Therefore, the current at X will also increase.

Figure 11(F) shows the condition which is most likely to give rise to dry-band arcing if the system is poorly designed. This was experienced during product development. For example, if zone 1 is very conductive (i.e. if R_r tends to metallic levels), the situation is unchanged from that of a wholly dielectric system; it is simply as if the clamp has been shifted up the cable. The parameter determining whether or not a damaging arc can form is the current, $i_{z\ wet}$, available if no gap were present, as in the case of Figure 11(E). If $i_{z\ wet}$ is kept sufficiently low any arc activity will not be severe enough to damage the cable, and so in this case we require:

$$i_{z\ wet} < 1 \text{ mA}$$

The limiting values used in this analysis are derived from many laboratory tests and installation measurements [9,20,27]. In applications to date, more conservative values have been used. A more detailed analysis is given in [28].

Table 2 shows some calculated values for typical geometry twin circuit towers. The analysis shows the impact of 50 m rods of 500 kΩ/m, and assumes pollution that gives a minimum resistance on the cable of 500 kΩ/m. The suspension location of the ADSS cable is close to that shown in Figures 1, 5 and 7. It should be noted that differential sag between conductors and the ADSS cable can significantly affect these values and so care must be taken with generalisation of such data. On this basis, if rods of R_r = 500 kΩ/m are used, the problem of dry-band arcing is overcome for a material able to withstand 1 mA. However, this is somewhat marginal for the 400 kV case, and if pollution levels have been under-estimated the system performance will be marginal.

REVIEW OF INSTALLATIONS OF THE ARC ARREST SYSTEM

To confirm the theoretical models and computer simulations, extensive trials were carried out at a location where the phenomenon of dry-band arcing was previously reliably produced (figure 3). This provided a situation where the damage to an unprotected cable could be reasonably predicted. Two 400 kV spans with high levels of salt fog were utilized. A high level of instrumentation was used to measure high and low frequency current on the cable. Also recordings of weather were also taken [20,24]. Figure 12 shows measurements made on an ADSS cable. The measured currents were very close to those predicted by the computation model used. Of particular interest are the periods of high current detected when single circuits were switched out, as seen repeatedly in May and again in July. In these periods the currents increase as phase cancellation from the two circuits no longer occurs (as shown in Figures 5 and 7). Also the base line currents are higher in June and July when rainfall is least. This is explained by an accumulation of salt on the cable during periods when there was no rain to wash it off, but fog was frequent. Towards the end of July rain cleans the cable and the current is reduced. Figure 13 shows measurements of currents which reveal arc activity on a cable. Adjacent spans were compared with and without rods attached. A continuous current of 1 mA is seen to be drawn by the rod. On the cable with no rod, significant 50 Hz and high-frequency currents can be seen at times of high humidity, indicating arcing activity. This period of time was one of unusually high activity. Regular inspections of the cable surface were carried out to correlate the condition of the cable with periods of arc activity.

One utility which installed a long route of polyethylene-sheathed ADSS cable, supplied by a number of companies, discovered damage associated with dry-band activity after only 6 months' installation (Figure 4). The original ADSS cable had been installed with a calculated background space potential of less than 12kV RMS for each tower type. This is below the safe installation limits described in specification IEEE P1222 [23]. However this cable is located in an area of very low rainfall and high levels of salt (from the sea) and industrial pollution. Lines of 110 kV and 220 kV system voltage are being used and both experienced problems of cable damage.

Calculations showed that the cable was exposed to very high currents because of the high levels of salt pollution and also the relative sags between the conductors and the optical cable. The situation was made worse by the use of a sheath which was not designed to resist dry-band arcing, thus a limit lower than 1 mA had to be set for acceptable arc currents. Figure 14 shows a typical calculation of the mid-span space potential and the current along the length of a span. Many such calculations were performed which showed that the rod was just able to provide a workable solution. For example, the effect of moving the suspension position of an ADSS cable on a single circuit 220 kV span is shown in Table 3. In this case the cable can be moved to a position B which reduces the currents on the cable if the relative sag of the conductors and the cables is only 9 m. If the differential sag is not controlled it is unlikely that the rod will always present a satisfactory solution. The analysis for 220 kV lines and 110 kV lines is similar since the distances between conductors tend to be in proportion to the voltages. In the event the above solution was deployed and the route continues to work. A detailed account of the installation and maintenance requirements is given elsewhere [29].

CONCLUSIONS

The retro-fit rod of controlled resistivity clearly has the potential to remove the threat of dry-band arc damage on ADSS cables. This is achieved by reducing the maximum current available on the cable for arcing activity. Rods can be applied to polyethylene sheathed cables or arc-resistant sheathed cables and can improve the performance of both.

Extensive trials in the UK have shown that the rod works, and have confirmed predictions of computer models. However, the engineering of the application of such as solution is complex. Individual spans of different geometry, including cable sag must be considered. In particular, local variation in pollution is critical and so knowledge of the proximity of the sea or industry must be considered. It is also very likely that areas which do not experience much rainfall will be particularly onerous since the cable will not be naturally regularly washed, so the pollution on its surface will tend to build up, reducing its resistance in times of high humidity, fog and dew.

ACKNOWLEDGEMENTS

The author would like to thank Corning Cable Systems for permission to publish the contents of this paper, and in particular Mr Malcolm Barnett for his faith in technology. This product would not exist without Steve Smith, Andy McDowell, Neil Haigh, Andy Platt and Ian Nichols.

REFERENCES

1 *Electric Cables Handbook*, 3rd Edition, Ed G. F. Moore, Blackwell Science 1997, Part 7, 'Optical Fibres in Power Transmission Systems,' Chapters 47-52, pp. 685-752.

2 S. C. Sharma, "Solution for fibre optic cables installed on overhead power transmission lines. A review," *IETE Technical Review*, vol. 11, pp. 215-222, 1994.

3 C. N. Carter, "Dry Band Electrical Activity on Optical Cables Strung on Overhead Power Lines", *Proc. 37th International Wire and Cable Symposium*, pp. 117-121, 1988.

4 C. N. Carter and M. A. Waldron, "Mathematical Model of dry-band arcing on self-supporting, all-dielectric optical cables strung on overhead power lines," *IEE Proc. C*, vol. 139, pp. 185-196, 1992.

5 G. G. Karady, G. Besztercey and M. W. Tuominen, "Corona caused deterioration of ADSS fiber-optic cables on high voltage lines," *IEEE Transactions on Power Delivery*, vol. 14, pp. 1438-1447, 1999.

6 C. .N. Carter, "Arc Controlling Devices for use on Self-supporting Optical Cables," *IEE Proc. A*, vol. 140, pp. 357-361, 1993.

7 U. H. P. Oestreich and H. M. Nassar, "Self-supporting dielectric fibre optical cables in high voltage lines," *37th Proc. International Wire and Cable Symposium*, pp. 79-82, 1988.

8 A. J. Peacock and J. C. G. Wheeler, "The development of aerial fibre optic cables for operation on 400 kV power lines," *IEE Proc. A*, vol. 139, pp. 304-313, 1993.

9 S. M. Rowland and F. Easthope, "Electrical ageing and testing of dielectric self-supporting cables for overhead power lines," *IEE Proc. A*, vol. 140, pp. 351-356, 1993.

10 F. Kaidanov, R. Munteanu and G. Sheinfain, "Damages and destruction of fiber optic cables on 161 kV overhead transmission lines," *IEEE Electrical Insulation Magazine*, vol. 16, pp. 16-23, 2000.

11 J. C. G. Wheeler, M. J. Lissenburg, and J. D. S. Hinchecliffe, "Advances in the development of aerial optic fibre cables," *6th BEAMA International Electrical Insulation Conference*, pp. 76-80, 1990.

12 J. C. G. Wheeler, M. J. Lissenburg, J. D. S. Hinchecliffe, and M. E. Slevin, "The development and testing of a track-resistant sheathing material for aerial optical fibre cables," *5th IEE Conference of Dielectric Materials Measurements and Applications*, pp. 73-76, 1988.

13 S. M. Rowland, "Sheathing materials for dielectric, aerial, self-supporting cables for application on high voltage power lines," *6th IEE Conference on Dielectric Materials, Measurements and Applications*, pp. 53-56, 1992.

14 S. M. Rowland and C. N. Carter "The evaluation of sheathing materials for an all-dielectric, self-supporting communication cable for use on long-span overhead power

lines," *5th IEE Conference on Dielectric Materials, Measurements and Applications*, pp. 77-80, 1988.

15 L. A. Dissado, M. J. Parry, S. V. Wolfe, A. T. Summers, and C. N. Carter, "A new sheath evaluation technique for self-supporting optical fibre cables on overhead lines," *39th Proc International Wire and Cable Symposium*, pp. 743-751, 1990.

16 R. Engle, S. Will and B. Wartschinski "Lifetime prediction of ADSS cables in high voltage environments," *49th Proc International Wire and Cable Symposium*, pp. 470-473, 2000.

17 M. J. Billings and K. W. Humphreys, "An outdoor tracking and erosion test of some epoxide resins," *IEEE Trans. EI*, vol. 3, pp. 62-70, 1968.

18 A. Bradwell, and J. C. G. Wheeler, "Evaluation of plastic insulators for use on British Railways 25 kV overhead line electrification," *IEE Proc. B, Electr. Power Appl.*, vol. 129, pp. 101-110, 1982.

19 A. G. W. M. Berkers, and J. M. Wetzwer, "Electrical stresses on a self-supporting metal-free cable on high voltage networks," *IEE Conf. on Dielectric Materials, Measurements and Applications*, pp. 69-72, 1988.

20 N. R. Haigh, S. M. Rowland, A. J. Taha, and C. N. Carter, "A fully instrumented installation and trial of a novel all-dielectric self-supporting cable system for very high voltage overhead power lines," *45th Proc. International Wire and Cable Symposium*, pp. 60-67, 1996.

21 Q. Huang, G. G. Karady, B. Shi and M. Tuominen, "Study on development of dry band on ADSS fibre optical cable", *IEEE Trans. DEI*, vol. 12, pp. 487-495, 2005

22 Q. Huang, G. G. Karady, B. Shi and M. Tuominen, "Numerical simulation of dry-band arcing on the surface of ADSS fibre optic cable", *IEEE Trans. DEI*, vol. 12, pp. 496-503, 2005.

23 IEEE draft Specification 1222P Standard for Self-Supporting Fibre Optic Cable (ADSS) for use on Overhead Utility Lines, 1995.

24 C. N. Carter, J. Deas, N. R. Haigh and S. M. Rowland, "Applicability of all-dielectric self-supporting cable system to very high voltage overhead power lines', *46th Proc. Int. Wire and Cable Symposium*, pp. 624-631, 1997.

25 S. M. Rowland and I. V. Nichols, GB19940021724, 'Combined electrical and optical power transmission system'.

26 A. J. Taha, I. V. Nichols, C. A. Platt and S. M. Rowland, "A novel system for the installation of all-dielectric self supporting optical cables on high voltage overhead power lines," *44th Proc. Int. Wire and Cable Symposium*, pp. 171-177, 1995.

27 S. M. Rowland and I. V. Nichols, "Effects of dry-band arc current on ageing of self-supporting dielectric cables in high fields," *IEE Proc. Sci. Meas. Technol*., vol. 143, pp 10-14, 1996.

28 S. M. Rowland, "Prevention of dry-band arc damage on ADSS cables" Accepted for publication in *IEEE Trans. DEI.*

29 S. M. Rowland, O. de la Cerda and N. R. Haigh, "Implementation of a solution to the problem of dry-band arcing on ADSS cables" Accepted for publication in *IEEE Trans. Power Delivery.*

TABLES

Space Potential Threshold Level (kV)	Cable Resistance per Unit Length (Ω/m)	Associated Pollution Level
10	200 k	Heavy
18	1 M	Medium
30	10 M	Light

Table 1. A typical heuristic used to determine 'safe' space potential in which an ADSS cable can be hung, as controlled by the environment of installation. An indication of the worst cable conductivity per unit length to be expected is also given [24].

System (kV)	R_r (kΩ/m)	R_c (kΩ/m)	$i_{x\,dry}$ (mA)	$i_{x\,dry}^2 R_r$ (W/m)	$i_{x\,wet}$ (mA)	$i_{xc\,wet}$ (mA)	$i_{x\,wet}^2 R_r$ (W/m)	$i_{x\,wet} R_r$ (V/m)	$i_{z\,wet}$ (mA)
400	500	500	2.9	4.2	3.4	1.7	5.8	1700	0.88
275	500	500	2.4	2.9	2.8	1.4	3.9	1400	0.69
132	500	500	0.72	0.26	0.83	0.42	0.34	415	0.20

Table 2. Comparison of spans of differing system voltages. In each case the resistive rod is 50 m long, and the span length 366 m.

					Position A		Position B	
	Span	Conductor sag	ADSS sag	Resistivity	$I_{z\,wet}$	$I_{xc\,wet}$	$I_{z\,wet}$	$I_{xc\,wet}$
	[m]	[m]	[m]	[kΩ/m]	[mA]	[mA]	[mA]	[mA]
1	450	16.5	13.2	500	0.09	0.46	0.37	0.34
2	450	16.5	13.2	1,000	0.07	0.31	0.21	0.20
3	450	9.0	9.0	500	0.29	0.51	0.10	0.14
4	450	9.0	9.0	1,000	0.17	0.33	0.05	0.09

Table 3. Calculations of current to determine the best location and relative sag for the ADSS cable.

FIGURE CAPTIONS

Figure 1. Typical location of ADSS cable on the lower cross-arm of a twin circuit tower

Figure 2. Schematic of the capacitive coupling between one phase conductor, the ADSS cable and the ground. Each conductor has an equivalent capacitance per unit length to the cable, C_L . The cable has a distributed capacitance to ground per unit length of C_G , and a resistance per unit length of R_l.

Figure 3. A photograph of cable damaged on a 400 kV line. The deep trough in the sheath is visible on the underside of the cable. The metallic wires on the left of the picture are part of the clamping system.

Figure 4. Damage on a polyethylene sheathed cable on a 110 kV line. The metallic wires on the left are part of the cable clamping system at the tower.

Figure 5. Space potential plots on a mid-span plane perpendicular to the conductors on a 400kV line. The contour intervals are 9.6 kV. Each contour is marked by the number by which 9.6 kV is to be multiplied to determine the space potential. The phase arrangement is ABC, CBA.

Figure 6. Measurements of current on an ADSS cable, on 400 kV line in polluted conditions. The lower levels of current represent the 50 Hz component and the dashed line shows higher frequency components implying periods of arc activity.

Figure 7. Space potential plot on a mid-span plane, perpendicular to the conductors for the span shown in Figure 5 with a single circuit outage. The contour intervals are 9.6 kV.

Figure 8. A schematic of the AAS rod on the ADSS cable. Conductors are not shown.

Figure 9. The AAS rods cover the regions of cable where significant currents can occur in the event of high pollution.

Figure 10. A simplified model of the arc arrest system rod on the cable.

Figure 11. Schematic showing the different conditions experienced by the system.

Figure 12. In each the case the graphs contain two traces from a 400 kV line. The higher trace represents the current measured on a 1.1 MΩ/m rod and the lower current represents the current measured on a 2.2 MΩ/m rod.

Figure 13. Current observed at times of arc activity (a) continuous 50Hz current on a span with rod attached, (b) high frequency current on control span with no rod, (c) 50 Hz current on the same control span, (d) relative humidity [24].

Figure 14. Predictions of space potential at mid-span, and current along the length of a half-span for a 110 kV single circuit line. The contours are multiples of 4 kV. The maximum current at the tower is 0.48 mA, and the current at the 50 m long rod tip is 0.12 mA.

FIGURES

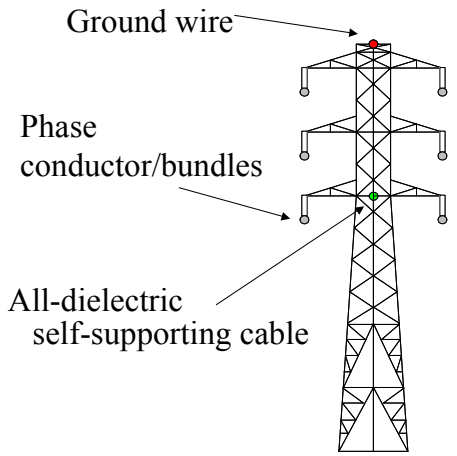

Figure 1.

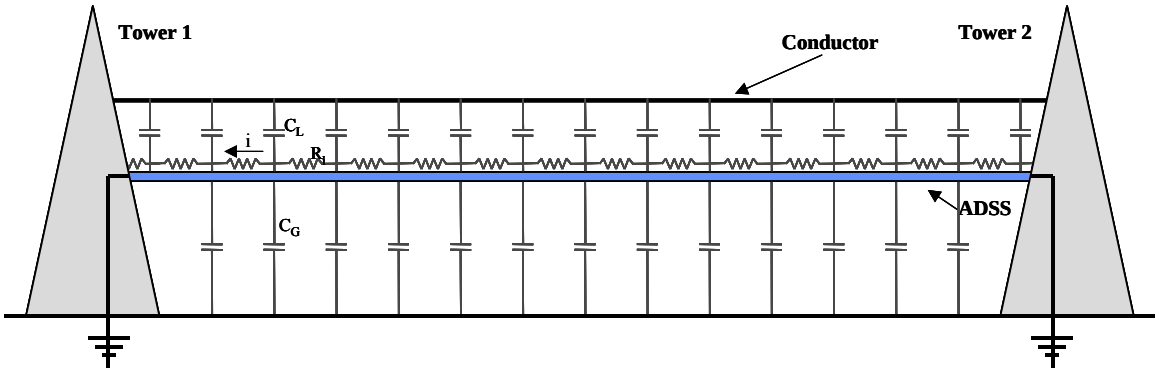

Figure 2.

Figure 3.

Figure 4.

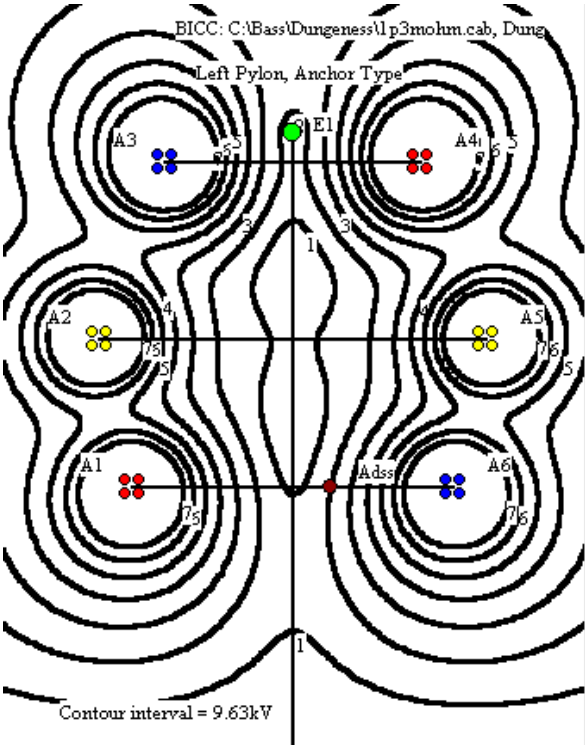

Figure 5.

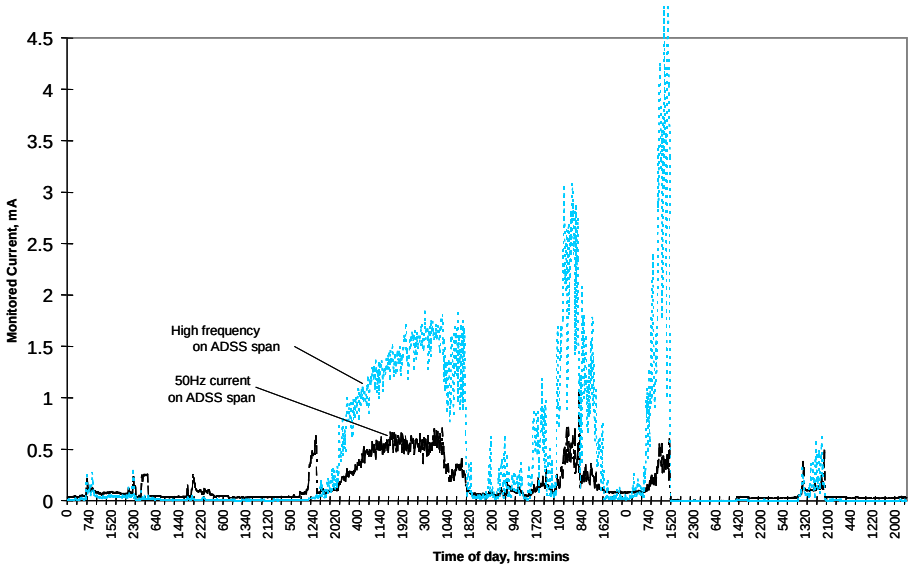

Figure 6.

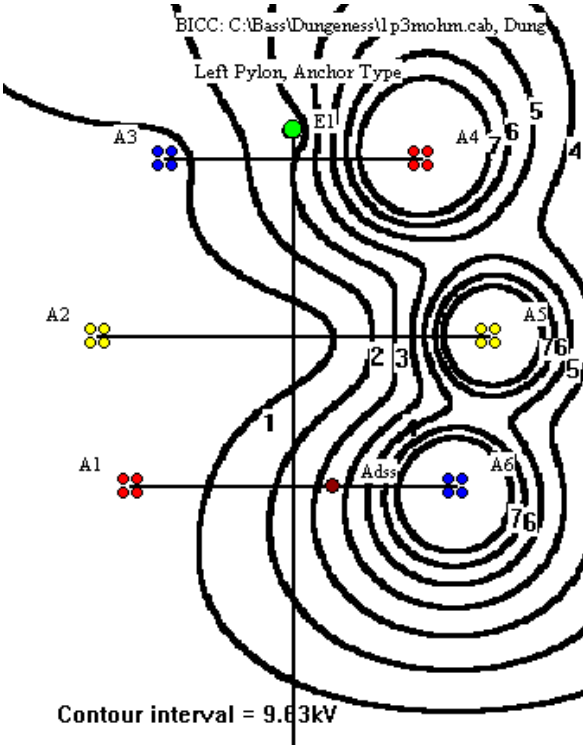

Figure 7.

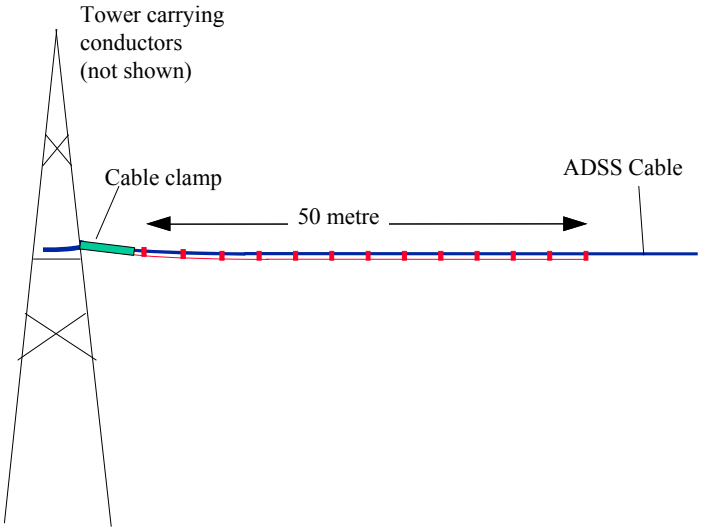

Figure 8

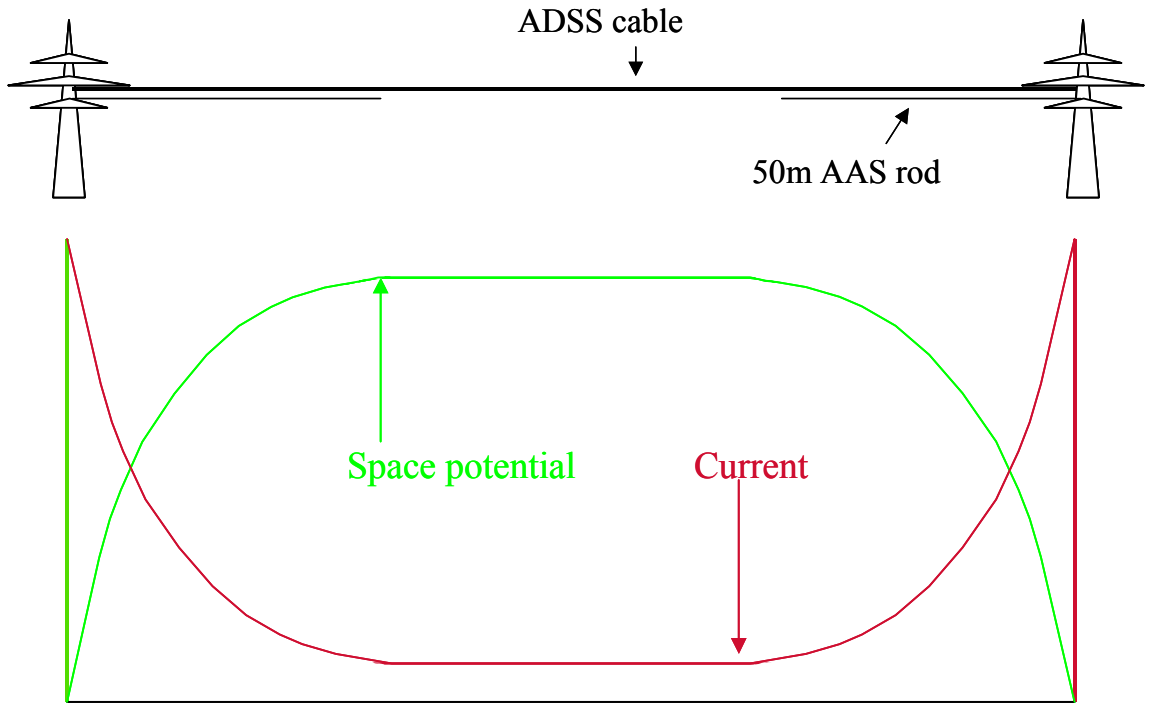

Figure 9

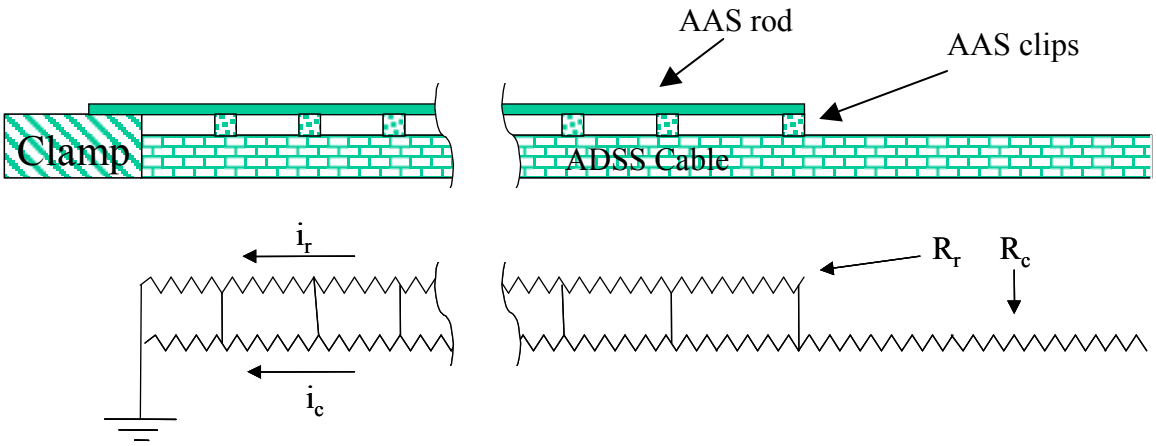

Figure 10

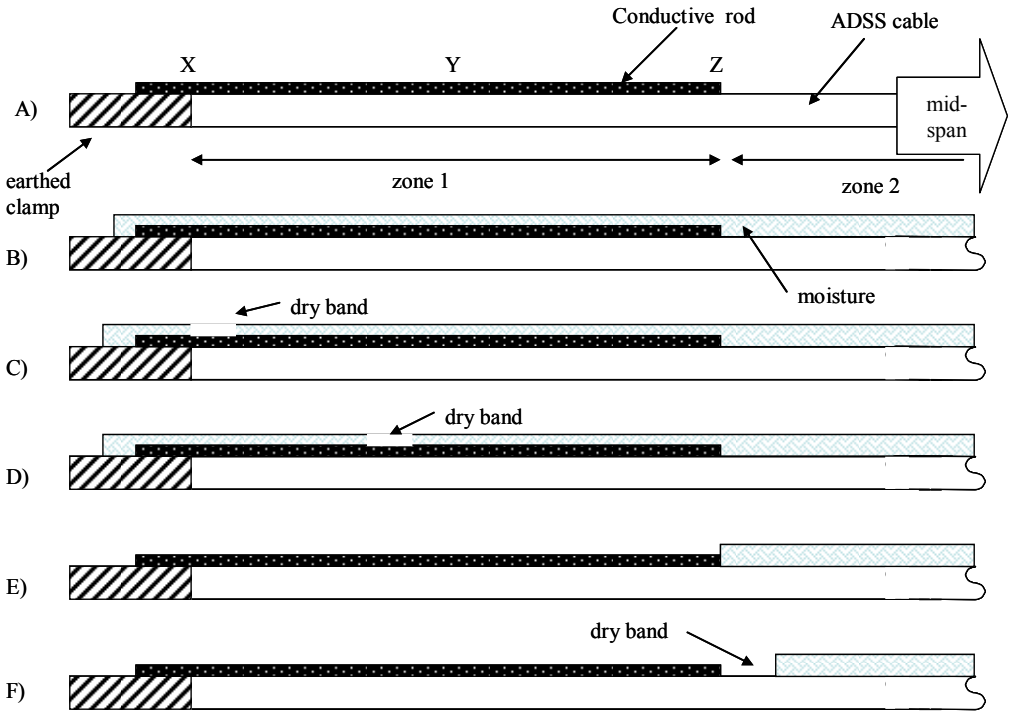
Conductive rod
ADSS cable
X
Y
Z
A)
mid-
span
earthed
clamp
zone 1
zone 2
B)
moisture
dry band
C)
dry band
D)
E)
dry band
F)

Figure 11.

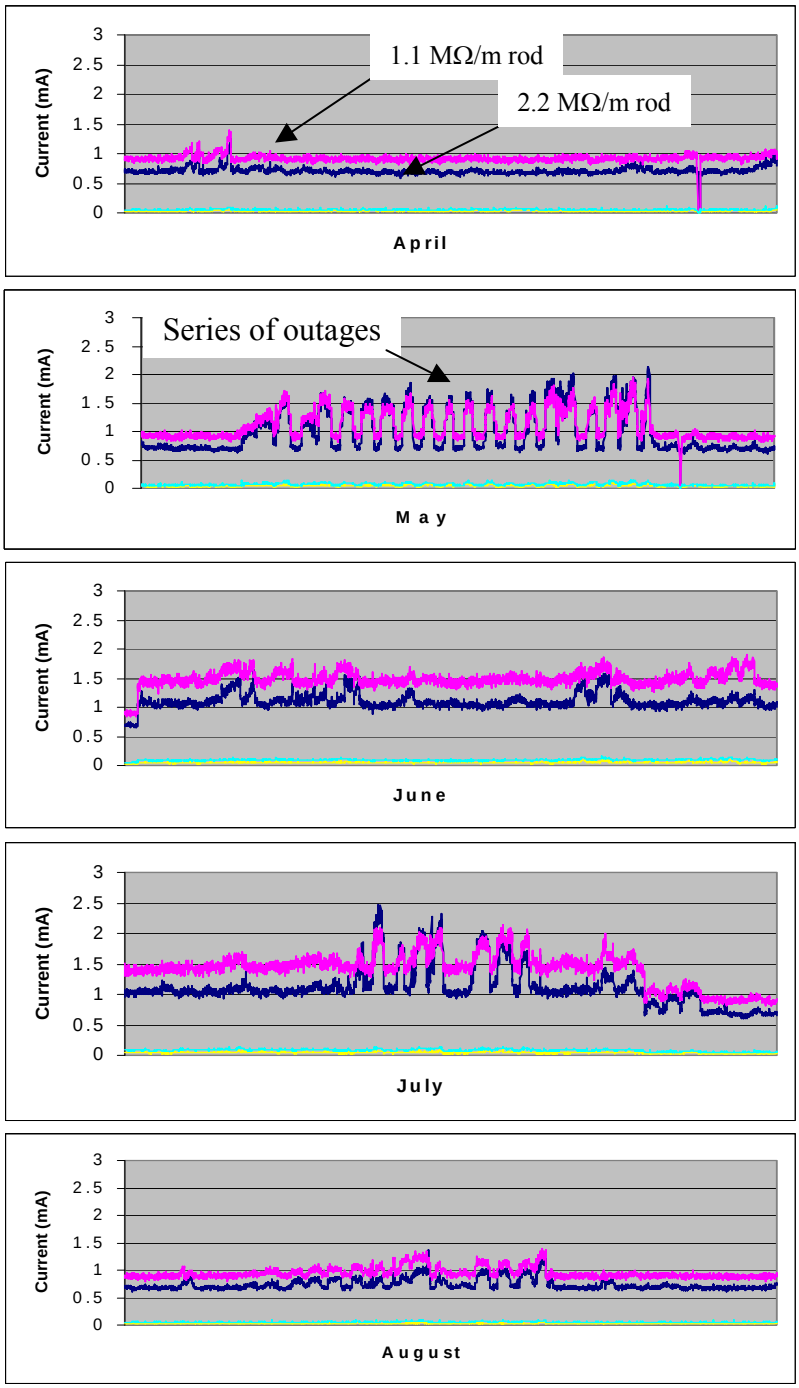
1.1 MΩ/m rod
2.2 MΩ/m rod
Current (mA)
April
Series of outages
May
June
July
August

Figure 12.

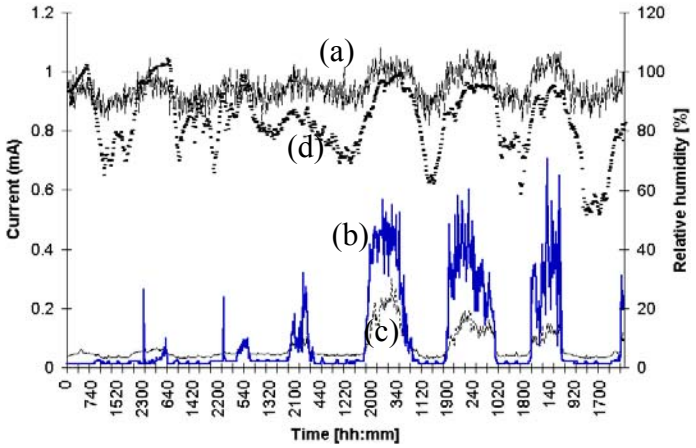

Figure 13.

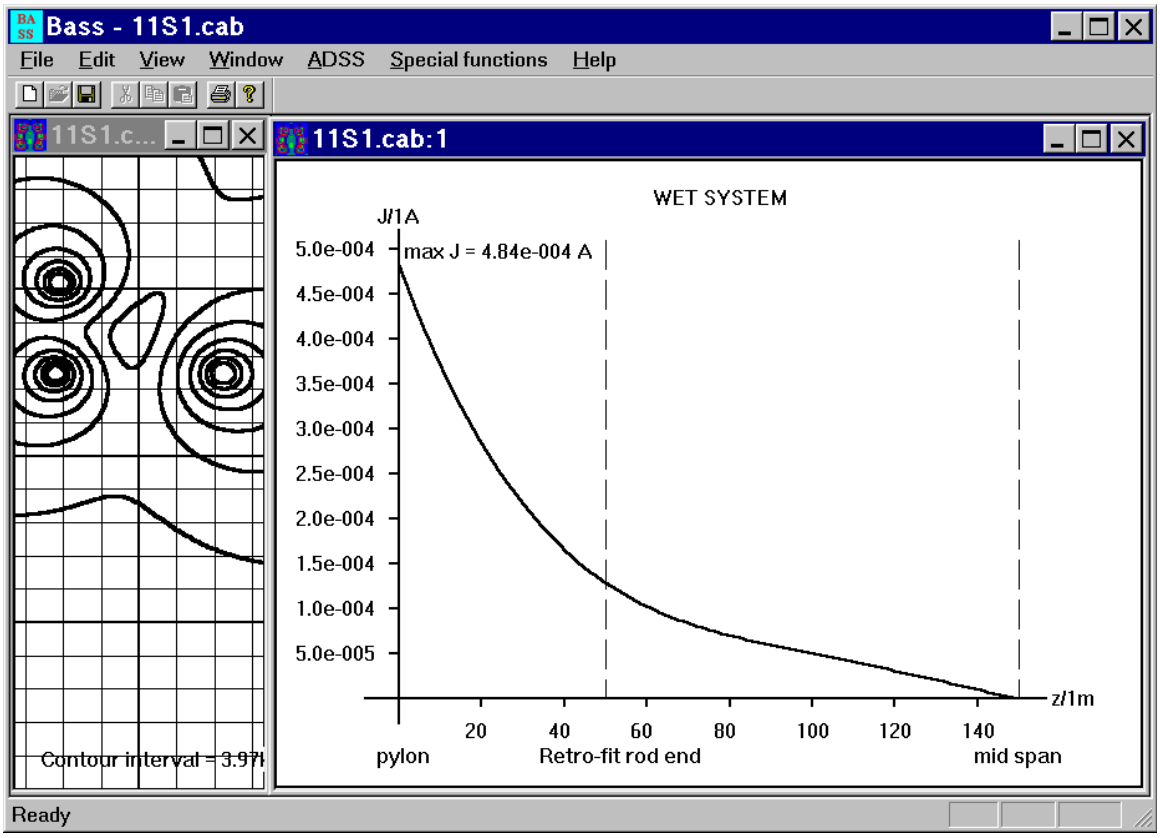

Figure 14.